Available online at www.sciencedirect.com

ScienceDirect

Procedia Manufacturing 47 (2020) 321–328

Procedia MANUFACTURING

www.elsevier.com/locate/procedia

23rd International Conference on Material Forming (ESAFORM 2020)

Monitoring of a Hammer Forging Testing Machine for High-Speed Material Characterization

Julen Agirre[a,*], Nagore Otegi[a], David Abedul[a], Angel Oruna[a], Lander Galdos[a]

[a]*Advanced Material Forming Processes research group, Mondragon Unibertsitatea, Loramendi 4, 20500 Arrasate-Mondragon, Spain*

* Corresponding author. Tel.: +34-687-001-422. *E-mail address:* jagirreb@mondragon.edu

Abstract

Dynamic testing of materials is necessary to model high-speed forming processes (i.e. hammer forging, blanking) and crash/impact behavior of structures, among others. The most common machines to perform medium to high-speed tests are the servo-hydraulic high-speed tensile and compression machines and the Hopkinson bars. The paper analyses the possibility to use a laboratory forging hammer for the characterization of materials at medium and high strain rates. For this, an automatized forging hammer has been constructed which is accelerated with a pneumatic cylinder and is able to speed up the upper anvil up to 5 m/s. This forging testing machine can be employed to perform a variety of material characterization tests, such as, uniaxial upsetting tests, plane strain compression tests as well as crash tests. To ensure the correctness of the experimental results obtained from tests performed in this home-developed laboratory facility, it is essential to verify and validate the acquired data. With this aim, copper cylindrical specimens have been deformed at different speeds. A high-speed camera has been employed to monitor real specimen strains using DIC and a load cell has been also utilized to measure the force applied during deformation. In order to obtain valid material rheological results, force data obtained from the load cell has been combined with DIC strain data to draw reference flow curves. Analogous stress-strain values have been calculated analytically using both techniques independently, solely high-speed camera data, on the one hand, and only load-cell data, on the other hand. A comparison of results has been performed and discussed in order to select the best monitoring technique to implement in the laboratory forging hammer.

Keywords: Forging; Material characterization; High-speed testing; Hammer; Monitoring

1. Introduction

Among all manufacturing processes, forging is a widely employed technology as it enables the production of parts with superior mechanical properties and with minimum material waste [1]. The initial billet, which usually has a simple geometry, is plastically deformed in one or more operations to produce parts with complex final geometries. The process is economically attractive when a large number of parts must be produced and/or when superior mechanical properties are required [1]. Frequently, such exceptional mechanical properties are achievable only by a forging process.

The type of press or hammer utilized for forging highly influences the forging process itself, as it affects the deformation rate and temperature conditions, as well as the production rate [1].

Focusing on the hammer, it is the least expensive and most versatile technology since it is capable of applying a wide range of loads and energies. Depending on the dimensions of the part and the capacity of the hammer, multiple impact blows may be required to obtain the final geometry [1]. Hammers are primarily used for hot and cold forging and by this process enhanced metallurgical properties of many materials can be achieved, including high-performance materials such as nickel-base superalloys used for many turbine disk applications [1,2].

It is well known that many process parameters have a big influence on the metallurgical properties of the final part and the deformation speed is one of the most remarkable ones.

10.1016/j.promfg.2020.04.260

Precisely, the most significant characteristic of hammers is the high deformation speed, thus, the high strain rates reached when forming the material. Strain rates in this type of processes could range from 10 up to 200 s^{-1}, while in press processes this variable could reach a maximum of 30 s^{-1} in the case of mechanical presses [3]. Strain rates in hydraulic presses do not exceed 10 s^{-1}.

Strain rate influences important process variables as the force needed to form the material and affects critical material transformation mechanisms, such as, the recrystallization phenomena. Recrystallization mechanisms are directly associated to the final grain size of the material, and therefore, the properties of the final product. On the one hand, regarding material hardening, the higher the strain rate the higher the force needed to deform the material, and on the other hand, as far as recrystallization phenomena are concerned, the higher the strain rate the finer the final grain size but also higher the critical strain required for recrystallization mechanisms to occur [4].

Even if the study of the aforementioned hardening and recrystallization phenomena in hammer conditions is of great industrial interest, few studies have been carried out and few materials have been tested in such high strain rates. One of the main reasons could be that very few commercial experimental testing facilities that allow hammer condition strain rates are available.

With this motivation, an automatic experimental forging simulator was developed and constructed. This laboratory-scale testing machine is capable of reproducing a wide range of real hot and cold industrial forging conditions, from low hydraulic press strain rates up to elevated hammer strain rates. Interestingly, additional forging strategies could be tested, such as, intermediate heating cycles and combined strain rate deformations.

In the present work, this home-developed forging testing machine was employed to perform high strain rate uniaxial upsetting tests at four different speeds. The tested material was a high purity copper. As far as data acquisition is concerned, two techniques were used. On the one hand, a high-speed camera was utilized to measure the kinematics of the upper die. By means of this technique, the true strain values of the flow curve were known. On the other hand, a load cell was employed to obtain force results. Combining the results of both acquisition techniques, reference flow curves were generated. Additionally, high-speed camera data and load cell data were independently used to analytically generate analogous flow curves. Finally, results of the three methods were compared and evaluated in order to select the best monitoring technique to implement in the experimental hammer testing machine.

2. Experimental forging testing machine

As mentioned in the introduction, very few commercial laboratory machines are capable of forging materials at hammer speeds (up 5 m/s or strain rates up to 200 s^{-1}). To cover that lack, a highly equipped experimental forging simulator was developed and constructed (Fig. 1). This laboratory-testing machine was designed to be able to perform different type of upsetting tests, as well as crash tests.

It is composed of four main sections: a heating furnace, a hydraulic press, a hammer and the final cooling system. To reduce human errors to the minimum extent, the machine is fully automated and the sample manipulation is carried out by an electro-pneumatic system integrated in the machine. In the following lines, each of the three sections are briefly explained and at the end of the section the main specifications of the testing facility are summarized (Table 1).

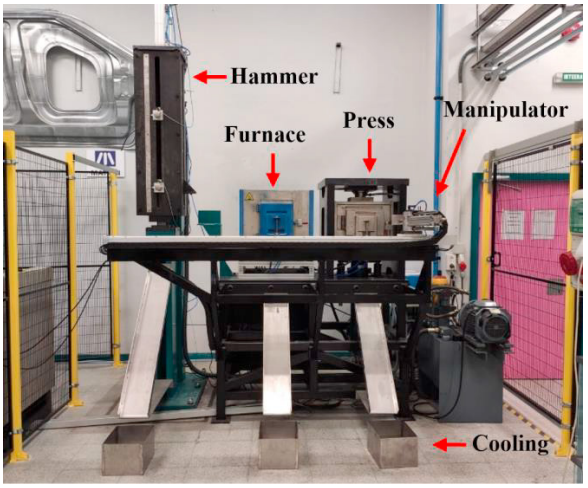

Fig. 1. Overview of the developed experimental forging simulator.

The heating furnace is an electric furnace with a maximum heating temperature of 1350 ºC. Interestingly, different heating cycles can be programmed, making this furnace ideal for initial and intermediate sample heating, as well as for all kind of heat treatments.

The hydraulic press gives the possibility to test the sample at low strain rates (0,01; 0,1 and 1 s^{-1}). The maximum applicable force is 25 t and it is important to mention that anvils are situated inside an electric furnace, which makes possible to perform isothermal experiments up to 1350 ºC.

The pneumatically actuated hammer is capable of performing high-speed deformations, up to 6 m/s. Such elevated speeds enable to perform tests at strain rates up to 300 s^{-1}, covering all the range of strain rates commonly reached in industrial hammer processes. In this case anvils are not preheated, as the contact time between the sample and the dies is very short. The weight of the anvils is of 92 kg and maximum applicable deformation energy and force are 1,5 kJ and 30 t, respectively.

The sample cooling system is based on three water tanks located in front of each heating/forming section. The sample manipulation system is optimized for the post-forming cooling to be as fast as possible in order to, for example, carry out accurate recrystallization parameter identification.

To finish with, four test modes are available: heat treatment mode, hydraulic press mode, hammer mode and combined (hydraulic press+hammer) mode. For the present work, only the hammer mode was employed.

Table 1. Main specifications of the experimental forging simulator

Machine section	Specification	Value
Heating furnace	Max. temperature	1350 ºC
Hydraulic press	Max. force	25 t
	Strain rates	0,001; 0,1; 1 s^{-1}
	Max. anvil temperature	1350 ºC
Hammer	Max. anvil speed	6 m/s
	Max. energy	1,5 kJ
	Strain rates	Up to 300 s^{-1}

3. Experimental procedure

With the objective of selecting the most appropriate acquisition technique to generate valid flow data at elevated strain rates, uniaxial compression tests at four different speeds were performed in the home-developed experimental forging simulator. Speed variation was carried out by modifying the falling height of the upper anvil.

Cylindrical samples (Ø15x22,5 mm) of high purity copper were employed for the research (Fig. 2). The use of copper in hammer-related tests is widely accepted since in 1962 Watermann succeeded on determining the blow energy of forging hammers by the copper-column upsetting method at Hannover Institute of Technology, Germany [5]. It is known that the strain rate sensitivity of high purity copper is very low, that is why it is an appropriate material to compare standard low-speed laboratory tests with hammer tests. As an example, Galdos et al. also used cylindrical samples of high purity copper for the characterization of an industrial hammer [6].

The uniaxial compression test is a widely well known method to determine the flow stress of a material as a function of the strain applied by compressing the cylindrical sample between two flat anvils [7]. Furthermore, this test is also widely employed to characterize the dynamic recrystallization (DRX) phenomena of metallic materials [4].

Even if a correct lubrication condition is of significant importance in order to obtain accurate compression flow data, in the present work neither lubrication nor Rastegaev-type samples were utilized [1]. The aim of the present work was not to obtain accurate flow curves of copper, but to evaluate different acquisition techniques. For the same reason, neither barreling nor temperature corrections were applied [8].

Fig. 2. Copper cylindrical samples utilized for the research

As far as data acquisition or monitoring is concerned, two techniques were utilized to acquire load and displacement experimental data. On the one hand, for the measurement of the kinematics of the upper die, an external Photron Fastcam-APX RS250K high-speed camera with appropriated illumination lamps was utilized (Fig. 3). This camera offers recording rates up to 250,000 fps, and for the present research experimental measurements were conducted at 15,000 fps. Random point-patterns were generated in the upper (moving) and lower (static) dies and by means of the Digital Image Correlation (DIC) software GOM Correlate, the true strain values of flow curves were obtained (Fig. 4).

On the other hand, a load cell was employed for the acquisition of the impact force (Fig. 3). This force sensor is mounted directly in the lower static anvil of the hammer and the acquisition frequency in the case of this technique was 300 kHz.

Combining the results of both acquisition techniques, reference flow curves were generated. Additionally, high-speed camera data and load cell data were independently used to analytically generate analogous flow curves. Finally, results of the three methods were compared and evaluated in order to select the best monitoring technique to implement in the experimental hammer testing machine.

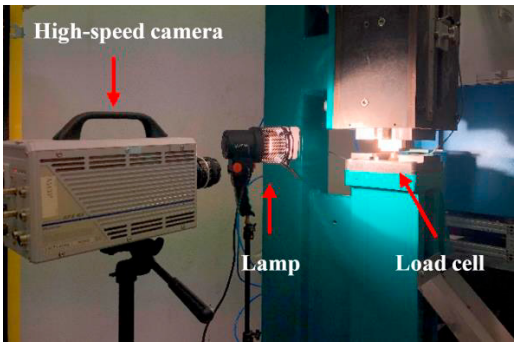

Fig. 3. Employed acquisition set-up.

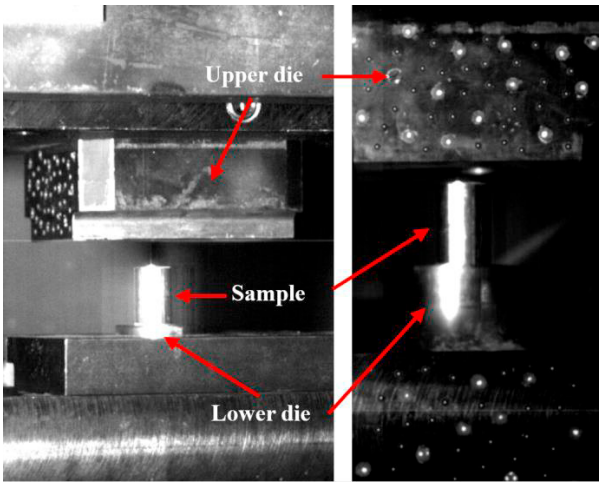

Fig. 4. Upper moving and lower static anvils recorded with Photron Fastcam-APX RS250K high-speed camera.

4. Results and discussion

In this section, experimental results are shown. First of all, reference flow curves are presented, which have been generated combining the strain obtained by the high-speed camera and the force measured by the load cell. Next,

analytically calculated flow curves using the high-speed camera data and the force sensor data independently are shown. Finally, a comparison of the three flow curves is presented.

Three repetitions were performed for each of the four velocities and a very low deviation was observed in all cases. In any case, mean values were calculated for each case. Undoubtedly, being the test automated enhances the repeatability of the results.

For the correct understanding of the results, during this section the lowest tested speed is referred as case 1, the next higher speed as case 2, the next higher speed as case 3 and the highest tested speed is referred as case 4.

4.1. Reference curves

As mentioned above, reference flow curves were generated combining the strain obtained by the high-speed camera and the force measured by the load cell.

As for high-speed camera results, Fig. 5 shows the DIC technique employed for the generation of the kinematic data of the upper and lower dies. A mean value of all the measured points was calculated in each case.

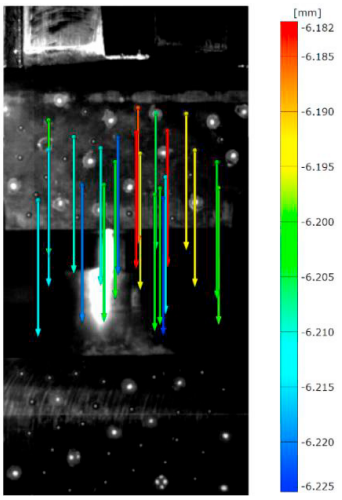

Fig. 5. Displacement of the upper die calculated with GOM Correlate DIC software.

Displacement and velocity data for each of the four cases is presented in Fig. 6. Logically, it is observed that higher the impact speed, higher the sample deformation. A displacement peak is observed at the beginning of each speed curve, at the instant at which the upper die contacts with the sample. This could be due to the lack of lubrication between both surfaces; therefore, the use of lubrication may smooth those peaks. It is also observed that the speed curves follow a relatively linear tendency.

It is important to highlight that the displacement of only the upper anvil was used to calculate reference true strain data, neglecting the displacement of the lower billet. In the most unfavorable case, the one of the highest velocity, the maximum displacement of the lower die was of 0,31 mm while the maximum displacement of the upper die was 11,67 mm. In the most unfavorable case, the displacement of the lower die is the 2,66 % of the displacement of the upper die.

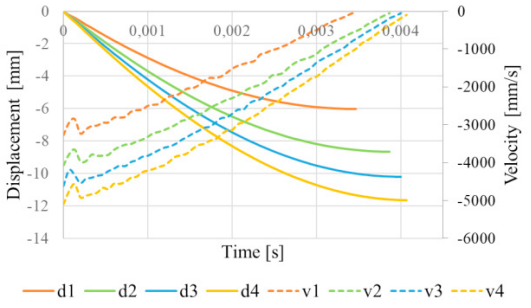

Fig. 6. Displacement and velocity of the upper die acquired with high-speed camera.

Fig. 7 shows the acceleration data of the upper die. Noise and little variation on acceleration values is observed from case to case.

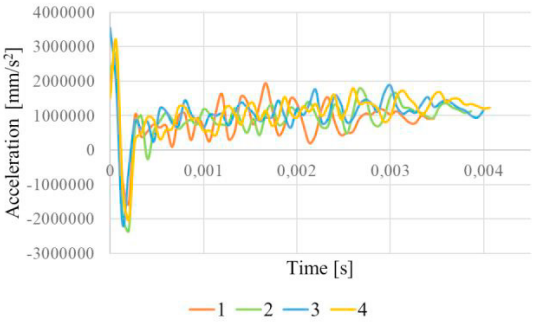

Fig. 7. Acceleration of the upper die acquired with high-speed camera.

To finish with data obtained by the high-speed camera, once calculated the true strain values taking into account the displacement, the true strain rate curves were calculated. It can be seen in Fig. 8 that at the highest speed, strain rates of almost 250 s^{-1} are reached, even if they tend to decrease with deformation. As mentioned in the introduction, in industrial hammer processes strain rates up to 200 s^{-1} are reached. Therefore, by the tests performed in the experimental forging simulator, all the range of strain rates reached in industrial hammers can be covered.

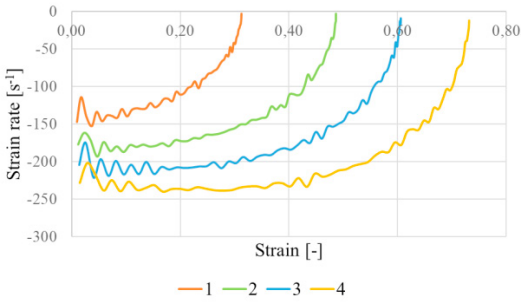

Fig. 8. Strain rates acquired with high-speed camera.

As far as the load cell is concerned, Fig. 9 shows the force acquisition during the performed compression tests. It can be seen that higher the strain rate, higher the force needed to deform the material.

As in the case of velocity data acquired by the high-speed camera, a peak is observed at the beginning of the test. This could be attributed to the first contact between the upper die and the sample and could be smoothed by applying lubrication between both surfaces. If that way peaks are not considerably flattened, some post-process mathematical smoothing could be recommendable. In the present work, non-smoothed raw data was employed in all the cases for the generation of reference flow curves.

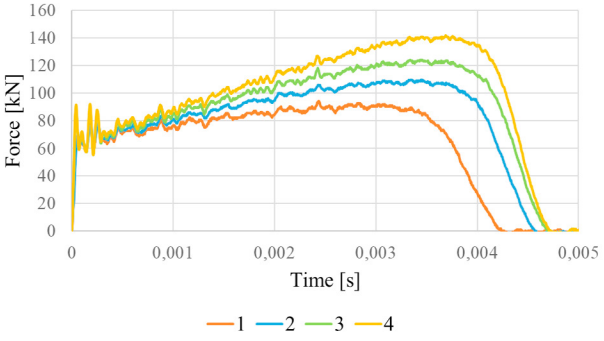

Fig. 9. Force data acquired with load cell.

Fig.10 shows force vs displacement curves generated combining the displacement acquired by the high-speed camera and the force acquired by the load cell. Additionally, a force vs displacement curve obtained from a compression test in a universal electro-mechanic drive Intron-4206 testing machine is shown. Compression test in the standard testing machine were performed at a strain rate of 0,001 s^{-1}, significantly lower strain rates than in the home-designed hammer testing machine. However, due to the low strain rate sensitivity of high purity copper, the difference in force is minimal.

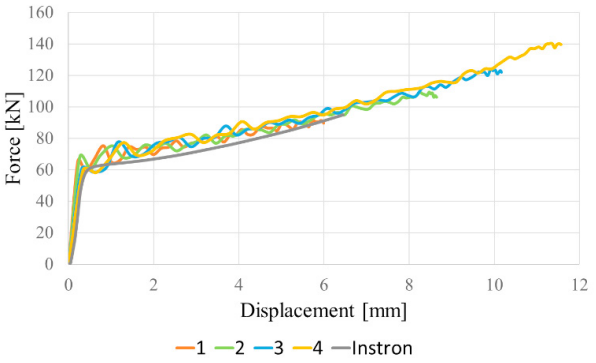

Fig. 10. Reference force vs displacement data.

To generate a typical stress strain curve, displacement values were converted into true strain values by the Eq. 1, and force values were converted into stress values by the Eq. 2:

$$\varepsilon = \ln\left(\frac{h}{h_0}\right) \tag{1}$$

$$\sigma = \frac{\vec{F}}{A} \tag{2}$$

where h and h_0 are the height of the sample at each point of the test and the initial height, respectively; and $\vec{F}$ and A are the force and transversal area at each point of the test, respectively.

Reference trues stress vs true strain flow curves are presented in Fig. 11. It is observed that high purity copper has a very low strain rate sensitivity, as increasing the strain rate stress values remain almost equal. That fact is also appreciated in the small stress difference among curves obtained in the laboratory hammer machine and the curve obtained in the standard Instron 4206 testing machine. Interestingly, a maximum true strain of almost 75 % was achieved at the highest strain rate.

Obtained flow curves show some noise, however, this noise could be mathematically smoothed if needed.

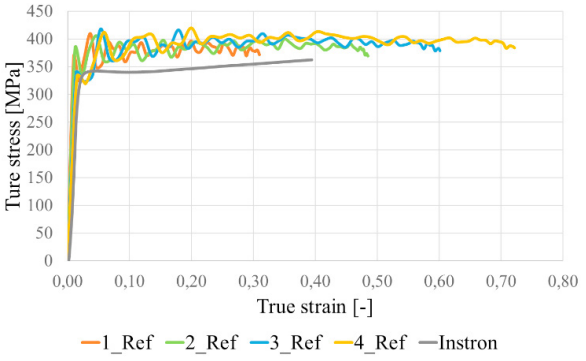

Fig. 11. Reference stress vs strain flow curves as well as Instron compression curves.

4.2. Curves employing uniquely high-speed camera data

Once the reference flow curves were obtained combining high-speed camera data and load cell data, a second approach was studied in order to evaluate its ability to calculate valid flow data in hammer conditions. For this second approach, the idea was to generate stress vs strain curves uniquely employing data acquired by the high-speed camera.

The utilized Photron Fastcam-APX RS250K high-speed camera is an expensive external device which is not integrated in the construction of the forging simulator. However, as in the case of the present research, it can be installed in the machine if required.

As presented in the previous section, employing the high-speed camera the kinematics of the upper and lower anvils could be directly acquired, therefore, the true strain is directly

obtained. To calculate force data out of the high-speed camera data, the Newton's second law was followed (Eq. 3):

$$\vec{F} = m \cdot \vec{a} \tag{3}$$

where m is the total mass of the moving elements and $\vec{a}$ is the acceleration acquired by the camera directly. It is known that the mass of all the moving elements is 88 kg.

As an example, for the case 3, force acquired by the load cell and the force calculated out of camera data is shown in the Fig. 12. Even if the calculated curve follows the reference tendency, significant noise can be appreciated. Moreover, at the beginning of the curve, at small strains, the calculated curve does not represent the reference curve.

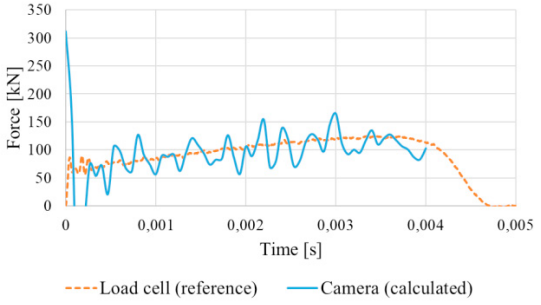

Fig. 12. Load cell (reference) force vs camera (calculated) force for the case 3.

Calculating the force in all the cases (Eq. 3) and converting it into stress (Eq. 2), stress vs strain curves were generated uniquely employing high-speed camera data (Fig. 13). Each case is presented separately as the noise makes difficult to differentiate them.

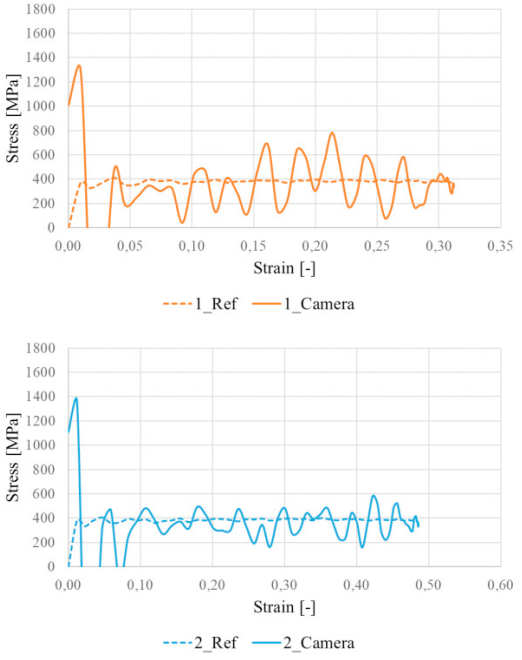

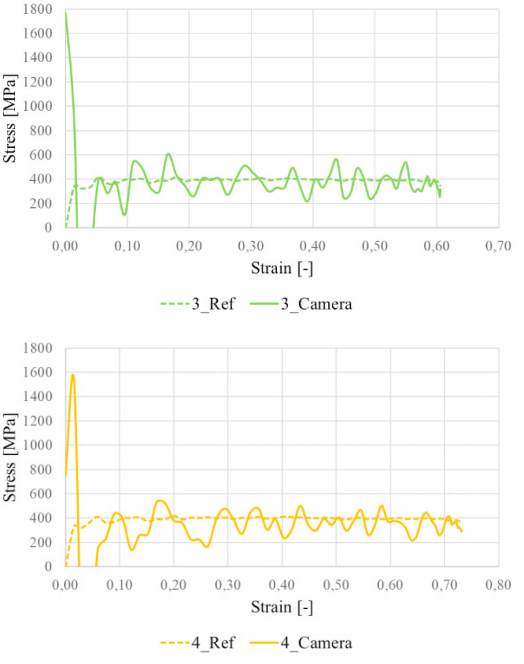

Fig. 13. Reference flow curves vs calculated (camera) flow curves for all the tested velocities.

Even if the calculated flow curves follow reference tendencies, significant noise is appreciated in all the cases. Besides, employing this monitoring technique, inability to represent the beginning of the flow curve at small strain is observed.

4.3. Curves employing uniquely load cell data

Finally, a third acquisition approach was analyzed. In this case the idea was to generate high strain rate stress vs strain curves uniquely employing data acquired by the load cell.

Unlike the high-speed camera, the load cell is integrated in the construction of the experimental forging simulator. Moreover, even if it is a high-priced device, it is not as expensive as a high-speed camera.

As presented in the previous section, utilizing the load cell deformation forces could be directly acquired. To calculate strain and stress data out of load cell data, first of all acceleration was calculated following the Newton's second law (Eq. 4):

$$\vec{a} = \frac{\vec{F}}{m} \tag{4}$$

where m is the total mass of the moving elements and $\vec{F}$ is the force acquired by the load cell directly. As mentioned previously, it is known that the mass of all the moving elements is 88 kg.

As an example, for the case 3, acceleration acquired by the high-speed camera and the acceleration calculated out of load cell data is shown in the Fig. 14. It is clearly appreciated that the calculated acceleration follows the reference tendency.

Furthermore, the calculated data is smoother than the data acquired by the high-speed camera, which is significantly more noisy.

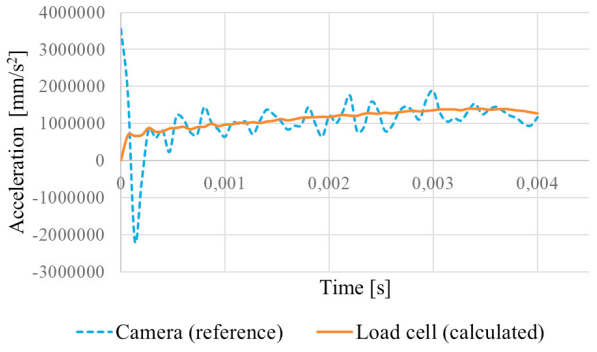

Fig. 14. Camera (reference) acceleration vs load cell (calculated) acceleration for the case 3.

Once calculated the acceleration at each point of the test, the equation of an accelerated linear motion was employed to calculate the position of the upper die at each point of the test (Eq. 5):

$$\vec{s} = \vec{s}_0 + \vec{v}_0 \cdot t + \frac{1}{2} \cdot \vec{a} \cdot t^2 \quad (5)$$

where $\vec{s}_0$ is the initial position of the upper die, $\vec{v}_0$ is its initial velocity, $\vec{a}$ is its acceleration and t is the time. To obtain position data by this equation, the initial velocity is the unique unknown among all the variables.

These data was obtained from the camera recordings but its calculation is easy by the use of two electric switches mounted the hammer.

Calculating the displacement in all the cases (Eq. 5) and converting it into stress and strain data (Eq. 1, 2), flow curves were generated utilizing uniquely load cell data (Fig. 15).

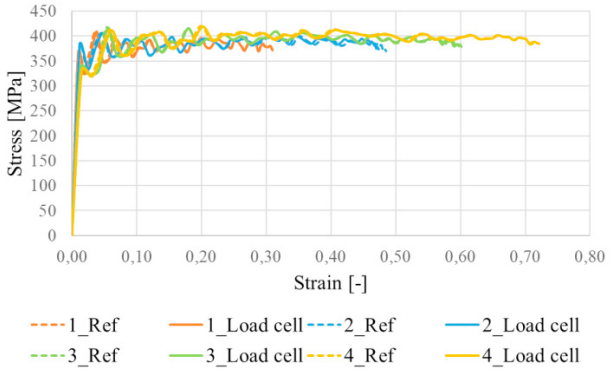

Fig. 15. Reference flow curves vs calculated (load cell) flow curves for all the tested velocities.

The calculated stress vs strain curves and reference flow curves show an excellent agreement. Similar noise is appreciated in both cases and the deviation between them is minimal.

4.4. Deformation energy

Additionally, deformation energies were calculated. Hammers are energy-restricted machines and during a working stroke, the deformation proceeds until the total kinetic energy is dissipated by plastic deformation of the material [1]. In a power-drop hammer, the total blow energy is generated by the free fall of the ram and by the pressure acting on the ram cylinder [1] (Eq. 6):

$$E = \frac{1}{2} \cdot m \cdot v^2 \quad (6)$$

where, m is the sum of the mass of all the moving elements and v is the velocity of the upper moving die just before the impact with the sample. Deformation energy results are presented in Table 2:

Table 2. Deformations energies for the four tested velocities

Impact velocity [m/s]	Deformation energy [kJ]
3,27	0,47
4,07	0,73
4,61	0,94
5,1	1,14

It is important to point that the design of the upper anvil of the hammer allows the addition of extra weights in order to reach higher deformation energies.

5. Conclusions

Finally, conclusions extracted in the present research work are listed below:

- A fully-automated experimental forging simulator was developed and constructed. This laboratory scale testing machine is capable of reproducing real industrial hot and cold forging conditions, from small to high strain rates. A hammer mode is available to perform tests at high strain rates (>200 s^{-1}).
- In the present work, high strain rate flow curves of high purity copper samples were obtained. For the generation of stress vs strain data, three data acquisition techniques were evaluated.
- A non-integrated high-speed camera was successfully utilized for the characterization of the kinematics of the hammer mode by the DIC technique.
- An integrated load cell was successfully employed for the force acquisition of the hammer.
- Reference flow curves were generated by combining high-speed camera strain data and load cell force data. Flow curves are logical and in good agreement with literature.
- Stress vs strain data calculated uniquely employing data acquired by the high-speed camera was not sufficiently accurate and noise is high to obtain accurate results.

- Stress vs strain data calculated uniquely employing data acquired by the load cell showed an excellent agreement to the reference flow curves. Therefore, it was concluded that this data acquisition technique will be implemented in the experimental forging simulator.

Acknowledgements

Authors would like to thank the Basque Government for the economic support given to the OGForge (Piezas forjadas de prestaciones extremas para el sector Oil & Gas mediante procesos de forja eficientes optimizados por modelos complejos de evolución microstructural) research project and the ULMA Forja S.Coop. company for the economic and technical support.

References

[1] Altan T, Ngaile G, Shen G. Cold and Hot Forging: Fundamentals and Applications. ASM International; 2005.
[2] Semiatin SL. ASM Handbook, Metalworking: Bulk Forming. vol. 14A. ASM International; 2005.
[3] Prasad YVRK, Rao KP, Sasidhara S. Hot Working Guide-A Compendium of Processing Maps. 2nd ed. ASM International; 2015.
[4] Huang K, Logé RE. A review on dynamic recrystallization phenomena in metallic materials. Mater Des 2016;111:548–74.
[5] Watermann D. Bestimmung des Arbeitsvermögens von Hämmern und Pressen mit Kupferzylindern. Werkstattstechnik, vol. 52; 1962. p. 95-101.
[6] Galdos L, De Argandoña ES, Herrero N, Ongay M, Adanez J, Sanchez M. The calibration of high energy-rate impact forging hammers by the copper-column upsetting method and high speed camera measurements. Key Eng Mater 2014;611–612:173–7.
[7] YE X jue, GONG X juan, YANG B biao, LI Y ping, NIE Y. Deformation inhomogeneity due to sample–anvil friction in cylindrical compression test. Trans Nonferrous Met Soc China 2019;29:279–86.
[8] Torrente G. Numerical and experimental studies of compression-tested copper: Proposal for a new friction correction. Mater Res 2018;21.